Int. J. Solids Structures Vol. 18, No. 7, pp. 597–609, 1982
Printed in Great Britain.

0020-7683/82/070597-13$03.00/0
Pergamon Press Ltd.

A CONSTITUTIVE EQUATION OF CREEP BASED ON THE CONCEPT OF A CREEP-HARDENING SURFACE

S. MURAKAMI and N. OHNO
School of Energy Engineering, Toyohashi University of Technology, Tempaku-cho, Toyohashi, 440 Japan

(*Received* 24 *April* 1981; *in revised form* 13 *October* 1981)

Abstract—A constitutive equation of creep for polycrystalline materials is developed by introducing a concept of a creep-hardening surface corresponding to the loading surfaces of plastic deformation. After discussing microstructural mechanisms of creep under reversed loading, it is first shown that the internal state of materials subject to creep can be described by a closed surface in creep strain space which specifies the strain range of the temporary softening of the materials (a creep-hardening surface), along with a strain point on or inside that surface. Then, by approximating the surface by a sphere of radius ρ and center α_{ij}, the constitutive equation of creep rate $\dot{\epsilon}^c_{ij}$ and the evolution equations for ρ and α_{ij} are formulated in analytical form. It is proved that the present theory coincides with the modified strain-hardening theory of the ORNL in its simplest case. Finally, the validity and the utility of the equations are discussed by comparing the numerical predictions with corresponding experimental results under non-steady and combined states of stress. The numerical results of the present theory are also compared with those of some constitutive equations of creep reported so far.

1. INTRODUCTION

Creep rate in the classical theory of creep is assumed to be specified as a function of the current states of stress and strain, the current temperature and the time elapsed after loading, and not to depend on the state of stress change[1–3]. However, in the case of stress reversal tests under constant magnitude of stress, a temporary increase in the creep rate is observed just after the stress change, and as creep proceeds the creep rate asymptotically approaches that of the creep-test without stress reversal[4–6]. The results of combined-stress tests under constant effective stress, furthermore, show that an abrupt rotation of the direction of the stress vector induces not only a transient non-coaxiality between the stress and the creep rate, but also a significant increase of the creep rate for a limited range of creep strain after the stress change[7–9]. These facts indicate that creep is an intrinsically anisotropic phenomenon governed by the past history of the deformation, or more specifically, that a change of the direction of the stress vector causes a transient softening of the material for a certain range of the succeeding strain. Since the deformation history generally can be represented by the strain trajectory in the creep strain space, the above phenomena, in turn, imply the existence of a certain closed surface in the creep strain space which specifies the range of temporary softening of the material, corresponding to the loading surfaces of plastic deformation[10–13].

So far a considerable number of constitutive equations have been formulated from metallurgical[4, 14, 15] or phenomenological[16–18] points of view to represent these anisotropic features of creep. However, though these theories succeeded to describe the creep behaviour under general states of stress to a certain extent, their mathematical structures are often too complicated to be employed in practical analyses of creep, and the determination of their material constants usually causes some additional difficulties. The Oak Ridge National Laboratory (ORNL), on the other hand, proposed an auxiliary rule for the classical strain-hardening theory of creep to formulate the creep behaviour under stress reversal conditions. This theory is quite ingenious, and has been frequently employed in recent analyses of creep because of its simplicity in notion as well as its feasibility to determine the material constants from conventional constant-stress creep tests. The ORNL theory, however, has a difficulty in that it does not always furnish a unique solution to a given problem, besides that it has not been expressed in analytical form. The lack of practical models capable of realistically describing creep behaviour under non-steady states of stress may be attributable to the fact that little effort has been made to represent the change of the internal state of materials due to creep from systematic view points of continuum mechanics and material science.

The present paper is concerned with the formulation of a new constitutive equation of creep for multiaxial and non-steady state of stress on the basis of the above notion of the

creep-hardening surface. The resulting equations are applied to the creep analysis of thin-walled tubes of type 304 stainless steel at 650°C subject to combined tension and torsion, and the numerical predictions are compared with the results of corresponding experiments to discuss the validity of the present theory.

2. CONSTITUTIVE ASSUMPTION AND ITS FORMULATION

2.1 *Constitutive equation of uniaxial creep under stress reversals*

The conventional strain-hardening theory of uniaxial creep[1–3] may be represented as follows:

$$\dot{\epsilon}^c = f(q, \sigma)\,\mathrm{sgn}\,[\sigma] \tag{1}$$

$$\dot{q} = |\dot{\epsilon}^c| \tag{2}$$

where $\dot{\epsilon}^c$ and σ denote the creep strain and the stress, and $\dot{(\cdot)}$ is a material derivative with respect to time t. Sgn [ ] in eqn (1), furthermore, stands for the sign of the bracketed argument. It is assumed in eqn (1) that the state of creep-hardening of the material is specified by a parameter q. Then q defined by eqn (2) increases monotonically irrespective of stress reversals, and represents progressive hardening of the material. When the sign of the stress changes under constant magnitude of stress as shown in Fig. 1(a), for example, eqns (1) and (2) predict a creep response shown by dashed lines OAC_3 and EE_1F of Fig. 1(b), (c), whereas the experimental results for various polycrystalline materials[4–8] show the creep behaviour like solid lines OAB_3 and EE_1E_7. Thus, the isotropic strain-hardening theory (1), (2) cannot describe realistically creep under reversed loading.

By examining the experimental results shown by the solid lines of Fig. 1(b), (c), it may be observed that:

(1) The change of the stress direction, or more directly the change of the direction in which creep proceeds, induces a temporary softening of materials, and the creep rate increases transiently;

(2) After a certain range of creep strain succeeding to the stress change, the creep rate attains to that of the creep tests without stress reversal; and

(3) The degree of the material softening depends on the magnitude of the strain caused by the preceding constant stress; the material softening is small as far as this preceding strain is small, whereas it becomes significant when the preceding strain is larger than a certain amount.

The results of multiaxial creep tests under constant effective stress[7, 8], furthermore, indicate that:

(4) The change of the principal stress direction brings about a transient non-coaxiality

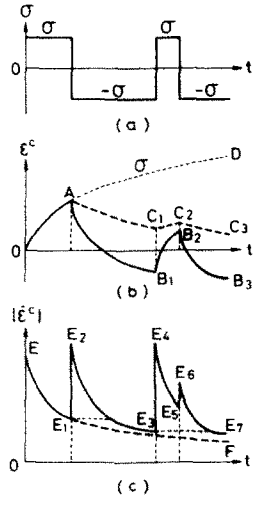

Fig. 1. Creep strain and creep rate under stress reversals.

between the creep rate and the stress tensor, along with a significant increase of the creep rate for a certain range of creep strain after the stress change.

These facts imply the existence of a certain creep bound in creep strain space which changes according to the development of creep and specifies the strain range of temporary softening of the material. We now discuss the evolution of this strain bound by examining predominant mechanisms of the microstructural changes in the material due to stress reversals for the uniaxial case, and develop a method to represent the hardening parameter q in terms of this strain bound.

As creep advances, dislocations generally lose their mobility due to their piling up to various obstacles or due to the formation of various networks, and induce the hardening of materials[4]. These immobilized dislocations may be divided into two parts; a reversible part which recovers mobility by stress reversals, and an irreversible part which has formed irreversible networks and does not recover the mobility. Thus when the direction of the stress is reversed, remobilization of the reversible part of dislocations induces a significant creep rate, which is attributable to the softening of the material. These remobilized dislocations move into the direction opposite to the previously immobilized one. Hence within a certain range of strain after the stress reversal, the reversible part of the dislocations will not form any irreversible structures. As the creep proceeds after the stress reversal, however, the remobilized dislocations are immobilized again gradually, and beyond this range of strain, they start to form irreversible dislocation networks.

Now let us consider a strain range inside which only reversible rearrangements of the dislocations take place as mentioned above, and call it *a range of recoverable creep-hardening.* When the creep strain ϵ^c proceeds under constant tensile stress σ_1 as shown in Fig. 2(a), the boundary of this range may develop as shown by the curves OA and OD in Fig. 2(b). By denoting the size and the center coordinate of this range by 2ρ and α respectively, it may be represented by a relation

$$g = (\epsilon^c - \alpha)^2 - \rho^2 \leqq 0. \tag{3}$$

The assumption mentioned above implies that the changes of irreversible dislocation structure occur only when the creep strain point ϵ^c is located on the boundary of the range. In this context, the bound $g = 0$ will be called *the creep-hardening bound.*

Let us now discuss a stress reversal from σ_1 to $-\sigma_2$ at time t_1. Since we have assumed that no changes of irreversible dislocation structures occur inside the strain range of eqn (3), the range of recoverable creep-hardening for $t_1 \leqq t < t_2$ remains unchanged, and is given by straight lines AB and DE in Fig. 2(b), where t_2 denotes the time when the creep strain attains to a point E on the boundary. For the time $t \geqq t_2$, furthermore, the creep-hardening bounds change again as shown by the curves BC and EF.

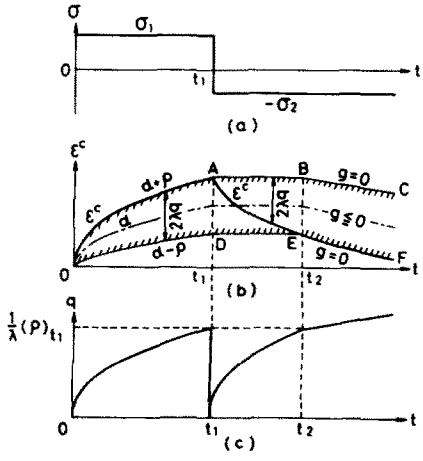

Fig. 2. Creep-hardening parameter and range of recoverable creep-hardening.

Thus, the range of recoverable creep-hardening expands, only when the creep strain point is on the creep-hardening bound and moves outward. Hence, the evolution of ρ is described by the following relation:

$$\dot{\rho} = \begin{cases} \lambda|\dot{\epsilon}^c|, & g = 0 \text{ and } (\partial g/\partial \epsilon^c)\dot{\epsilon}^c > 0 \quad (4a) \\ 0, & g < 0 \text{ or } (\partial g/\partial \epsilon^c)\,\dot{\epsilon}^c \leqq 0 \quad (4b) \end{cases}$$

where λ is a material constant specifying the rate of increase of ρ. In view of eqn (3), we have a relation $dg = 0$ when $g = 0$ and $(\partial g/\partial \epsilon^c)\dot{\epsilon}^c > 0$. Substitution of eqn (4a) into this relation readily yields the evolution equation of α as follows:

$$\dot{\alpha} = \begin{cases} (1-\lambda)\dot{\epsilon}^c, & g = 0 \text{ and } (\partial g/\partial \epsilon^c)\dot{\epsilon}^c > 0 \quad (5a) \\ 0, & g < 0 \text{ or } (\partial g/\partial \epsilon^c)\dot{\epsilon}^c \leqq 0. \quad (5b) \end{cases}$$

We are now in a position to discuss the change of the creep-hardening parameter q. There are no stress reversals on the curve OA of Fig. 2(b). Hence, by assuming that the classical strain-hardening theory applies on this curve, eqns (2) and (4a) provide

$$q = |\epsilon^c| = (1/\lambda)\rho, \qquad (0 \leqq t < t_1). \quad (6a)$$

When the stress changes from σ_1 to $-\sigma_2$ at time t_1, the parameter q decreases instantaneously owing to the remobilization of reversible dislocations. We assume, in this case, that the density of the remobilized dislocations is sufficiently large, and the creep rate $\dot{\epsilon}^c$ just after the stress reversal can be approximated by that of eqn (1) substituted from $q = 0$. Thus q decreases instantaneously to zero at $t = t_1$, and increases thereafter as the creep proceeds, as shown in Fig. 2(c). Since the remobilized dislocations do not form any irreversible networks in the interval $t_1 \leqq t < t_2$, the state of creep-hardening at $t = t_2$ is equal to that just before the stress reversal as observed in Fig. 2(c). Then, if the increase of q in the range of recoverable creep-hardening is assumed to be proportional to the change of ϵ^c, q may be given as follows:

$$\begin{aligned} q &= (1/2\lambda)|\epsilon^c - (\alpha + \rho)| \\ &= (1/2\lambda)\rho - (1/2\lambda)(\epsilon^c - \alpha) \qquad (t_1 \leqq t < t_2) \end{aligned} \quad (6b)$$

where eqn (3), namely, the relation $\rho \geqq |\epsilon^c - \alpha|$ has been employed. For the time $t \geqq t_2$, furthermore, ϵ^c is located on the creep-hardening bound and moves outward. Therefore it may be assumed that the classical strain-hardening theory applies just as on the curve OA. Hence q at $t \geqq t_2$ may be given as follows:

$$\begin{aligned} q &= |\epsilon^c(t_1)| + |\epsilon^c(t) - \epsilon^c(t_2)| \\ &= (1/\lambda)\rho \qquad (t \geqq t_2). \end{aligned} \quad (6c)$$

Equation (6a–c) can be unified by the following consideration. For times $0 \leqq t < t_1$ and $t \geqq t_2$, σ and $(\epsilon^c - \alpha)$ are of the same sign, and the condition $g = 0$ holds. For $t_1 \leqq t < t_2$, on the other hand, they have different signs until ϵ^c attains to the center of the range $g \leqq 0$, while they are of the same sign thereafter. In view of this relation, eqns (6a–c) can be expressed by a single relation

$$q = (1/2\lambda)\rho + \operatorname{sgn}[\sigma(\epsilon^c - \alpha)](1/2\lambda)|\epsilon^c - \alpha|. \quad (6d)$$

Though eqn (6d) has been derived for tension followed by compression, it applies to a general history of uniaxial loading; e.g. to compression followed by tension, or when a stress reversal occurs while ϵ^c is located inside the range $g \leqq 0$. Equation (6d) implies that a stress reversal generally induces an instantaneous change of q by an amount $(1/\lambda)|\epsilon^c - \alpha|$, and that the strain-history dependence of the creep rate is expressed in terms of $(\epsilon^c - \alpha)$.

Thus, eqn (6d) constitutes a constitutive equation of uniaxial creep together with eqn (1). As observed from eqn (6d), the parameter q has a discontinuity at $\sigma = 0$. Hence, when the stress approaches instantaneously zero and oscillates between very small positive and negative values, the parameter q shows discontinuous jumps from one value to another. However, such discontinuous jumps of q do not cause any discontinuity in the material response, if we assume that the constitutive function $f(q, \sigma)$ in eqn (1) *et seq.* may be zero and continuous at $\sigma = 0$.

In the particular case of $\lambda = 0$, the above equations lead to the classical strain-hardening theory of eqns (1) and (2). If we take $\lambda = 1/2$, on the other hand, eqns (1), (3)–(5) and (6d) are reduced to the following form:

$$\dot{\epsilon}^c = f(q, \sigma)\,\mathrm{sgn}\,[\sigma] \tag{7a}$$

$$q = \rho + \mathrm{sgn}\,[\sigma(\epsilon^c - \alpha)]|\epsilon^c - \alpha| \tag{7b}$$

$$\dot{\rho} = \begin{cases} (1/2)|\dot{\epsilon}^c|, & g = 0 \text{ and } (\partial g/\partial \epsilon^c)\dot{\epsilon}^c > 0 \\ 0\ , & g < 0 \text{ or } (\partial g/\partial \epsilon^c)\,\dot{\epsilon}^c \leqq 0 \end{cases} \tag{7c}$$

$$\dot{\alpha} = \begin{cases} (1/2)\dot{\epsilon}^c, & g = 0 \text{ and } (\partial g/\partial \epsilon^c)\dot{\epsilon}^c > 0 \\ 0\ , & g < 0 \text{ or } (\partial g/\partial \epsilon^c)\,\dot{\epsilon}^c \leqq 0 \end{cases} \tag{7d}$$

$$g = (\epsilon^c - \alpha)^2 - \rho^2. \tag{7e}$$

The quantities $\epsilon^- = \alpha + \rho$ and $\epsilon^+ = \alpha - \rho$ specified by eqns (7c, d) represent, respectively, the maximum and the minimum value which ϵ^c has taken so far. Then, eqn (7b) may be written in an alternative form.

$$q = \begin{cases} |\epsilon^c - \epsilon^+|, & \sigma \geqq 0 \\ |\epsilon^c - \epsilon^-|, & \sigma < 0 \end{cases} \tag{8}$$

and eqn (7) is reduced to the modified strain-hardening theory of ORNL [3, 5]. It should be noted, however, that eqn (7) is expressed in analytical form without recourse to strain origins ϵ^+ and ϵ^-. Thus we can formulate more elaborate and more convenient constitutive equations of creep by extending the creep-hardening range into multiaxial states of stress.

As observed from the above argument, when the change of stress sign occurs on the bound $g = 0$, eqn (6d) or (7b) gives $q = 0$ and the creep rate may become instantaneously infinite, which implies an instantaneous change of inelastic strain. Therefore, it should be noted that, though the above equations are concerned with creep strain, they may be applicable also to predict the instantaneous plastic response under transient loading conditions.

2.2 *Constitutive equation of creep for multiaxial and non-steady states of stress*

We begin with the generalization of eqn (3) into multiaxial states of stress. As mentioned in the preceding section, the range of recoverable creep-hardening represents a strain range in which the motion of remobilized dislocations induces creep strain but does not form any irreversible dislocation structures. Since it is easiest for the remobilized dislocations to move into the direction opposite to their previous motion, the range of recoverable creep-hardening in a multiaxial state of stress is the largest in the direction of reversed straining, and will have a form shown schematically by a dashed line in Fig. 3. However, if the strain-histories do not deviate significantly from proportional or reversed loading, the range of recoverable creep-hardening may be approximated by a sphere

$$g = (2/3)(\epsilon_{ij}^c - \alpha_{ij})(\epsilon_{ij}^c - \alpha_{ij}) - \rho^2 \leqq 0 \tag{9}$$

as shown in Fig. 3, where α_{ij} is a deviatoric tensor of rank two.

The range of recoverable creep-hardening defined by eqn (9) expands and translates only when the creep strain point ϵ_{ij}^c is located on the surface $g = 0$ and moves outward. Hence $\dot{\rho}$ and $\dot{\alpha}_{ij}$

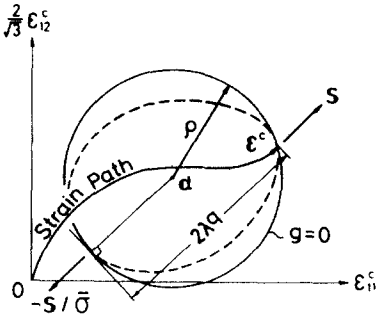

Fig. 3. Creep-hardening surface in multiaxial state of stress.

of eqns (4) and (5) will be extended to multiaxial states of stress as follows:

$$\dot{\rho} = \begin{cases} \sqrt{(2/3)}\lambda \dot{\epsilon}^c_{ij} n_{ij}, & g = 0 \text{ and } (\partial g/\partial \epsilon^c_{ij})\dot{\epsilon}^c_{ij} > 0 \\ 0\ , & g < 0 \text{ or } (\partial g/\partial \epsilon^c_{ij})\dot{\epsilon}^c_{ij} \leqq 0 \end{cases} \tag{10}$$

$$\dot{\alpha}_{ij} = \begin{cases} (1-\lambda)\dot{\epsilon}^c_{kl} n_{kl} n_{ij}, & g = 0 \text{ and } (\partial g/\partial \epsilon^c_{ij})\dot{\epsilon}^c_{ij} > 0 \\ 0\ , & g < 0 \text{ or } (\partial g/\partial \epsilon^c_{ij})\dot{\epsilon}^c_{ij} \leqq 0 \end{cases} \tag{11}$$

where n_{ij} is defined as

$$n_{ij} = (\epsilon^c_{ij} - \alpha_{ij})/[(\epsilon^c_{kl} - \alpha_{kl})(\epsilon^c_{kl} - \alpha_{kl})]^{1/2} \tag{12}$$

and denotes the unit outward normal vector to the surface $g = 0$. In the derivation of eqn (11), we have used the consistency condition $dg = 0$ together with the assumption that the surface translates in the direction n_{ij}. The particular case of $\lambda = 1/2$ of eqns (10)–(12) corresponds to the evolution equations employed by Chaboche *et al.*[19] to describe the cyclic plastic behaviour of metallic materials. However, they defined these equations *a priori*, and did not make any physical interpretation.

Let us now specify the creep-hardening parameter q. As already observed in Fig. 2(c), q in uniaxial creep decreases to zero at the instant of stress reversal due to the effect of the remobilized dislocations. In multiaxial states of stress, however, active slip planes will alter according to the rotation of the principal stress direction, and the value of q will decrease also due to the corresponding softening of the material. In other words, even when the creep strain point ϵ^c_{ij} is located on the surface $g = 0$ and moves outward, q may become less than $(1/\lambda)\rho$ which corresponds to the hardening state under simple loading, if s_{ij} and $(\epsilon^c_{ij} - \alpha_{ij})$ are not collinear. Such a hardening variable q, therefore, can be specified by generalizing eqn (6d) into the following form:

$$q = (1/2\lambda)[\rho + (\epsilon^c_{ij} - \alpha_{ij}) s_{ij}/\bar{\sigma}] \tag{13a}$$

$$\bar{\sigma} = [(3/2) s_{ij} s_{ij}]^{1/2} \tag{13b}$$

where the second term of eqn (13a) represents the history dependence of q. It can be shown that $2\lambda q$ is equal to the distance between the creep strain point ϵ^c_{ij} and the tangential plane of an outward normal vector $-s_{ij}/\bar{\sigma}$, Fig. 3. Thus, creep-hardening of materials is specified by the configuration of the surface $g = 0$ together with the current state of creep strain. In this context, the surface $g = 0$ will be referred to as *the creep-hardening surface* hereafter, and may be compared with the loading surfaces of plastic deformation[10–13].

By assuming the collinearity between the creep rate $\dot{\epsilon}^c_{ij}$ and the deviatoric stress tensor s_{ij}, eqn (1) may be readily generalized as follows:

$$\dot{\epsilon}^c_{ij} = (3/2) f(q, \bar{\sigma}) s_{ij}/\bar{\sigma} \tag{14}$$

where $f(q, \bar{\sigma})$ is zero and continuous at $\bar{\sigma} = 0$ as discussed previously. Refinement of eqn (14) by taking account of the non-coaxiality between $\dot{\epsilon}_{ij}^c$ and s_{ij} will be discussed in the next section.

2.3 *Further elaboration of the theory*

As observed in Fig. 5 discussed later, while the creep rate immediately after the stress reversal is considerably larger than that of undeformed matrial after the loading, the creep rate decreases rapidly as creep advances. We now elaborate the preceding theory by incorporating such a change of creep rate along with the non-coaxiality between the creep rate tensor and the deviatoric stress tensor mentioned above.

The significant and temporary increase of the creep rate after the stress reversal is caused partly by an anelastic recovery of creep strain due to the action of the back stress, besides the remobilization of the immobilized dislocations[4]. Although there have been considerable works[4, 15–18] to formulate constitutive equations of creep by taking account of such a back stress, they are not always successful from practical point of view. However, this effect may be described also by non-linearizing the term $(\epsilon_{ij}^c - \alpha_{ij})$ in eqn (13), because the results of Fig. 5 imply that, while the creep-hardening parameter q does not increase significantly for a while after the stress reversal, it starts to increase rapidly as the creep strain point traverses the range of recoverable creep-hardening. Such a change of q may be represented by revising eqn (13) as follows:

$$\left.\begin{aligned} q &= (\rho/\lambda)[\mu/(2\rho)]^{\zeta} \\ \mu &= \rho + (\epsilon_{ij}^c - \alpha_{ij}) s_{ij}/\bar{\sigma} \end{aligned}\right\} \tag{15}$$

where ζ ($\geqq 1$) is a material constant. When the creep strain point is located on the creep-hardening surface and $(\epsilon_{ij}^c - \alpha_{ij})$ is collinear with s_{ij}, in particular, eqn (15) leads to $q = (1/\lambda)\rho$ and $\mu = 2\rho$, and is independent of the parameter ζ. Thus, the effect of non-linearity in $(\epsilon_{ij}^c - \alpha_{ij})$ is largest just after the stress reversal or just after the change of the principal stress direction, and vanishes gradually.

Though the collinearity between $\dot{\epsilon}_{ij}^c$ and s_{ij} has been assumed in the derivation of eqn (14), these tensors are generally non-coaxial in the case of non-proportional loading. This non-coaxiality occurs as a result of the disparity between the principal direction of the stress tensor and that of the internal state variable, and is most significant immediately after the change of the principal stress direction. This implies that the principal direction of the internal state variable draws gradually toward that of the deviatoric stress tensor after the stress change.

As the internal state can be described by $(\epsilon_{ij}^c - \alpha_{ij})$ in this theory, the above argument means that the creep rate $\dot{\epsilon}_{ij}^c$ occurs so that $(\epsilon_{ij}^c - \alpha_{ij})$ may become coaxial with s_{ij}. The coaxiality between $(\epsilon_{ij}^c - \alpha_{ij})$ and s_{ij} may be established most quickly when the creep strain ϵ_{ij}^c changes toward $\bar{\epsilon}_{ij}^c$ in Fig. 4 along the dashed line, where $\bar{\epsilon}_{ij}^c$ is a point on the creep-hardening surface located in the direction of s_{ij} starting from the center α_{ij} of the surface, and may be given as

$$\bar{\epsilon}_{ij}^c = \alpha_{ij} + (3/2)\rho s_{ij}/\bar{\sigma}. \tag{16a}$$

Though the creep rate $\dot{\epsilon}_{ij}^c$, in this case, is directed in the direction of $(\bar{\epsilon}_{ij}^c - \epsilon_{ij}^c)$, the direction of

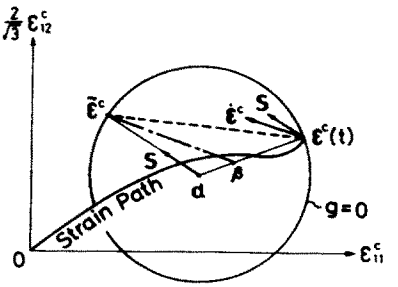

Fig. 4. Non-coaxiality between creep rate tensor and deviatoric stress tensor.

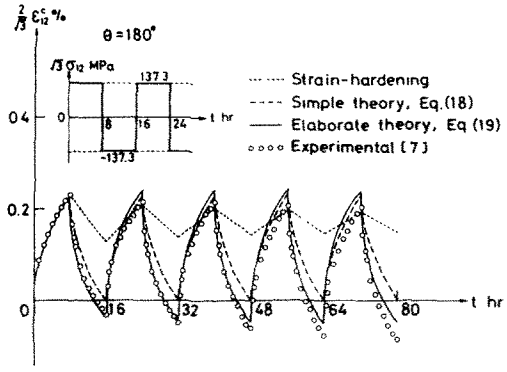

Fig. 5. Creep strain under reversed torsion ($\theta = 180°$).

$\dot{\epsilon}_{ij}^c$ generally deviates from this one to that of s_{ij}. Hence, in view of the collinearity of s_{ij} and $(\tilde{\epsilon}_{ij}^c - \alpha_{ij})$, $\dot{\epsilon}_{ij}^c$ may be specified as collinear with a tensor $(\tilde{\epsilon}_{ij}^c - \beta_{ij})$, where β_{ij} is a point of certain interior division between ϵ_{ij}^c and α_{ij}. Thus, eqn (14) may be revised as follows:

$$\dot{\epsilon}_{ij}^c = \sqrt{(3/2)} f(q, \bar{\sigma})(\tilde{\epsilon}_{ij}^c - \beta_{ij})/[(\tilde{\epsilon}_{kl}^c - \beta_{kl})(\tilde{\epsilon}_{kl}^c - \beta_{kl})]^{1/2} \tag{16b}$$

$$\beta_{ij} = \alpha_{ij} + \xi[1 - q/(\rho/\lambda)](\epsilon_{ij}^c - \alpha_{ij}) \tag{16c}$$

where ξ is a material constant which represents the degree of non-coaxiality caused by the change of the principal stress direction.

Equations (9)–(14) may be further extended to include the phenomena of the anelastic creep recovery mentioned above only by introducing the back stress η_{ij}, and by replacing s_{ij} of eqn (14) by the corresponding quantity $(s_{ij} - \eta_{ij})$ [15–18].

3. COMPARISON WITH EXPERIMENTAL RESULTS AND DISCUSSION

Let us now elucidate the characteristics and the validity of the present theory by analyzing the multiaxial creep subject to rotation of principal stress directions, and by comparing the numerical results with those of the ORNL theory as well as of the corresponding experiment. The experiments were performed under combined tension and torsion at 650°C on type 304 stainless steel tubes [7].

The numerical analyses were performed by the classical strain-hardening theory given by eqns (1) and (2), the anisotropic constitutive equations of the present theory given by eqns (9)–(14) with $\lambda = 1/2$, and by those combined with eqns (15) and (16). These equations are summarized as follows:

$$\left.\begin{aligned} \dot{\epsilon}_{ij}^c &= (3/2) m A^{1/m} q^{(m-1)/m} \bar{\sigma}^{(n-m)/m} s_{ij} \\ q &= \int_0^t [(2/3)\dot{\epsilon}_{ij}^c \dot{\epsilon}_{ij}^c]^{1/2} \, \mathrm{d}t \end{aligned}\right\} \quad \text{(strain-hardening)} \tag{17}$$

$$\left.\begin{aligned} \dot{\epsilon}_{ij}^c &= (3/2) m A^{1/m} q^{(m-1)/m} \bar{\sigma}^{(n-m)/m} s_{ij} \\ q &= \rho + (\epsilon_{ij}^c - \alpha_{ij}) s_{ij}/\bar{\sigma} \end{aligned}\right\} \quad \text{(simple theory)} \tag{18}$$

$$\left.\begin{aligned} \dot{\epsilon}_{ij}^c &= \sqrt{(3/2)} m A^{1/m} q^{(m-1)/m} \bar{\sigma}^{n/m} [F_{ij}/(F_{kl}F_{kl})^{1/2}] \\ q &= 2\rho[1/2 + (\epsilon_{ij}^c - \alpha_{ij}) s_{ij}/(2\rho\bar{\sigma})]^{\xi} \\ F_{ij} &= (3/2)\rho s_{ij}/\bar{\sigma} - \xi[1 - q/(2\rho)](\epsilon_{ij}^c - \alpha_{ij}). \end{aligned}\right\} \quad \text{(elaborate theory)} \tag{19}$$

The values of ρ and α_{ij} in eqns (18) and (19) are given by eqns (10) and (11) substituted from $\lambda = 1/2$. In the case of simple tension under a constant stress, in particular, eqns (17)–(19) reduce to an identical expression

$$\epsilon^c = A\sigma^n t^m. \tag{20}$$

Thus, the material constants involved in eqns (17)–(19) are given as follows:

$$\left.\begin{aligned} &A = 3.1 \times 10^{-19}\ (\text{hr})^{-0.54}(\text{MPa})^{-7.2}, \quad m = 0.54, \quad n = 7.2 \\ &\zeta = 2.1, \quad \xi = 0.25 \end{aligned}\right\} \tag{21}$$

where A, m and n were determined from the results of torsional creep tests under constant stress $\sqrt{(3)}\sigma_{12} = 117.7$, 137.3 and 156.9 MPa. The constant ζ, furthermore, was determined by fitting eqn (19) to the creep curves following stress reversals in the reversed torsion test shown in Fig. 5, whereas ξ was determined so that the non-coaxiality between $\dot{\epsilon}^c_{ij}$ and s_{ij} in Fig. 6 might be described by eqn (19).

Equations (18) and (19) predict the infinite creep rate at the instant of a stress reversal, since the parameter q becomes zero upon change of the stress sign. Thus, there may arise a question whether the creep strain rates given by eqns (18) and (19) tend to zero when the stress has changed its sign but still remains very close to zero. However, it can be easily proved that eqn (18), for example, gives the expression $|\epsilon^c(t) - \epsilon^c(t_1)| = A|\sigma_c|^n(t - t_1)^m$ for constant compression σ_c following tension and for time $t \geqq t_1$, where t_1 denotes the time of the stress reversal. Thus, it will be seen that $|\epsilon^c(t) - \epsilon^c(t_1)|$ becomes zero as $|\sigma_c| \to 0$. This implies that the above question concerning the continuity of material response is guaranteed. This holds true in the case of eqn (19) as well.

3.1 *Comparison between predictions of present theory and results of experiment*

Figures 5–8 show the results of the present theory for repeated multiaxial loading histories entered in the figures, together with the results of the corresponding experiment. The changes in the principal stress direction are $\theta = 180$, 150, 90 and 30° where the angle θ formed by two

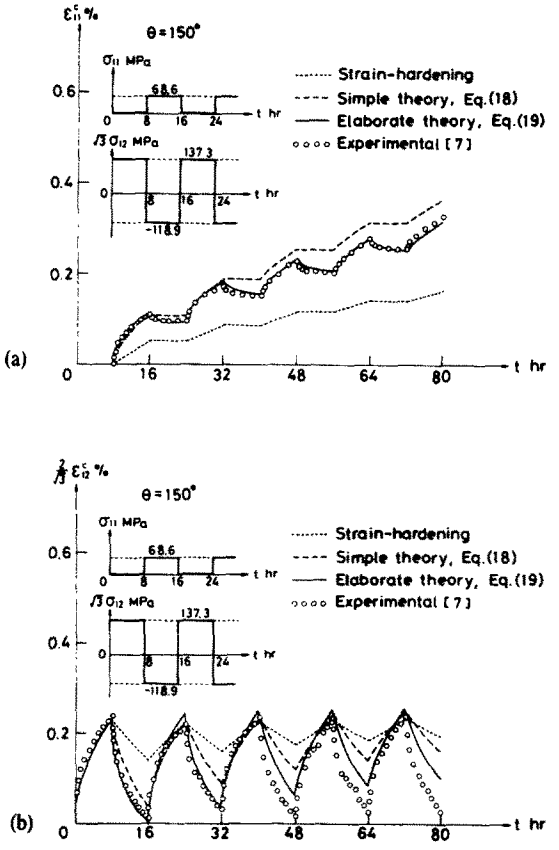

Fig. 6. Creep strain under cyclic multiaxial loading ($\theta = 150°$).
(a) Axial creep strain. (b) Torsional creep strain.

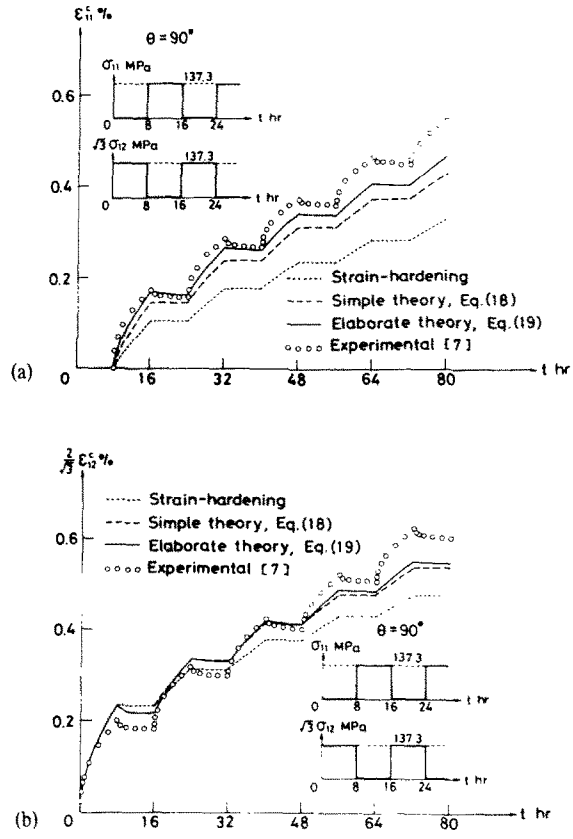

Fig. 7. Creep strain under cyclic multiaxial loading ($\theta = 90°$).
(a) Axial creep strain. (b) Torsional creep strain.

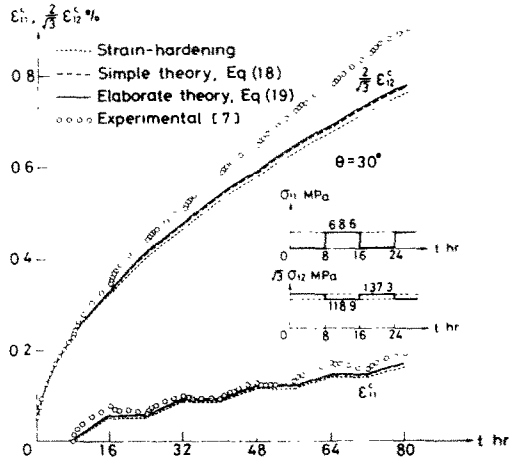

Fig. 8. Axial and torsional creep strain under cyclic multiaxial loading ($\theta = 30°$).

different states of the deviatoric stress s_{ij} and s^*_{ij} is defined as follows:

$$\cos\theta = s_{ij}s^*_{ij}/(s_{kl}s_{kl}s^*_{mn}s^*_{mn})^{1/2}. \tag{22}$$

The dashed and solid lines in these figures are predictions of eqns (18) and (19), whereas the dotted lines show the results of the classical strain-hardening theory of eqn (17).

In the case of alternating torsion $\theta = 180°$ in Fig. 5, experimental creep curves after each stress reversal show considerably larger creep rate than that of the initial loading, and the

maximum and the minimum strain in each cycle decreases gradually as the stress cycle proceeds. It will be observed that these features can be described very well by the elaborate theory of eqn (19). Though the results of the simple theory, eqn (18), show some local deviation from the experiment, it gives fairly good predictions, especially for the upper peak strains in each cycle, and may be a significant improvement to the classical strain-hardening theory.

Figure 6 (a, b), on the other hand, shows the results of $\theta = 150°$. While the results of the elaborate theory (eqn 19) coincide almost completely with the experiment in the case of axial strain ϵ_{11}^c, they tend to show somewhat smaller strain amplitudes than the experiment in the case of torsional strain ϵ_{12}^c. This may be accounted for by the fact that the angle formed by $(\epsilon_{ij}^c - \alpha_{ij})$ and s_{ij} after stress reversals decreases as the number of cycles increases, and therefore the amount of decrease in q caused by each stress reversal diminishes gradually.

The results of the simple theory (eqn 18) for axial creep strain ϵ_{12}^c represented by the dashed line in Fig. 6(a), on the other hand, show some deviation from the experimental results, and the difference between them amounts to about 20%. Similar trends are observed also for torsional creep strain ϵ_{12}^c in Fig. 6(b). However, these deviations are much smaller than those between the classical strain-hardening theory and the experiment. Moreover, in view of the simplicity of the expression as well as the fact that it requires no additional material constants other than usual creep data, eqn (18) may be a useful constitutive equation for routine analyses of engineering creep problems.

Similar comparisons for the case of $\theta = 90°$ are shown in Fig. 7 (a, b). In the argument of Section 2.2, we restricted the stress-histories to those of nearly proportional or nearly reversed loading. However, it will be observed from this figure that both versions of the present theory describe the experimental results with fairly good accuracy, and hence the present theory is applicable even to stress-histories deviating from proportional or reversed loading. After the first stress rotation by $\theta = 90°$, eqns (18) and (19) give an abrupt decrease of q by factors of 1/2 and $(1/2)^\zeta$, respectively. Thus, the present theory represents the temporary softening of the material just after the first stress rotation. As the number of cycles increases, however, some deviations are observed between the predicted and experimental creep rates just after stress rotations. This may be attributable to the effect of the anelastic creep strain which was disregarded in the present theory, see Section 2.3. It must be noticed, however, that these deviations of creep rates vanish rapidly as creep proceeds after stress rotations, and will be insignificant if the period of stress rotation is not so short.

Figure 8 shows the results for the case of $\theta = 30°$. In this case, the differences in the results of eqns (17)–(19) are immaterial, and they all describe the experimental results sufficiently well.

3.2 *Discussion to the* ORNL *theory*

Finally, let us make a brief discussion to the modified strain-hardening theory of the ORNL. As mentioned previously, this theory may sometimes give non-unique predictions, in addition to that it is not expressed in analytical form and hence its algorithm in the computation is rather complicated. Figure 9(a, b) shows the prediction due to the ORNL theory for the same stress history as that of Fig. 6. The dotted lines in this figure indicate the results of the ORNL theory calculated strictly for the stress history shown in the figure, while the dashed lines again show the results of the ORNL theory but calculated by extending the interval of the stress change at each time by a small amount of time Δt (that is, $8, 8 + \Delta t, 8 + 2\Delta t, \ldots$ hr). The latter corresponds also to the case where the stress levels are increased by a small amount at each time of stress change. Since the difference between these two stress histories is essentially insignificant, the two results should not have any noticeable differences. The results of the dotted and the dashed line however, differ markedly as observed in the figure. These results, furthermore, show considerable deviation from the experiment and the corresponding predictions of the simple version of the present theory entered by the solid lines in the figure.

4. CONCLUSION

A new constitutive equation of creep under multiaxial and non-steady states of stress was first formulated by specifying a creep-hardening surface in creep strain space. In case of a simple state of stress, the modified strain-hardening theory of the ORNL is recovered as a special case of the present theory.

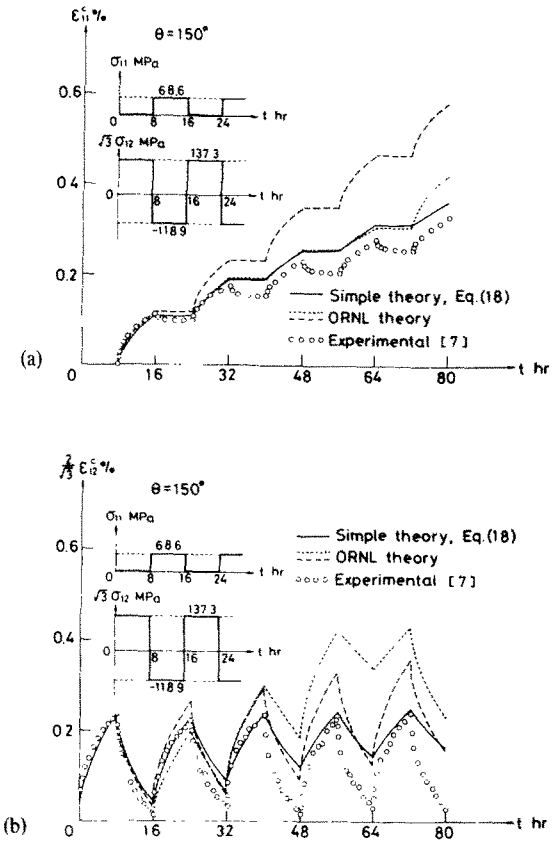

Fig. 9. Predictions of the ORNL theory for cyclic multiaxial loading ($\theta = 150°$).
(a) Axial creep strain. (b) Torsional creep strain.

Then, torsional creep under stress reversal as well as multiaxial creep under combined tension and torsion and subject to cyclic rotation of the principal stress direction were analyzed by the resulting equations. The validity and the utility of the present theory were discussed by comparing the theoretical results with those of the corresponding experiments on type 304 stainless steel tubes at 650°C. It was elucidated that the ORNL theory may sometimes give non-unique predictions, in addition to that its algorithm for computation is rather complicated. However, the constitutive equations (9)–(16) or (18) and (19) developed in this paper do not have these difficulties, and give better predictions to creep behaviour under a general state of stress. Furthermore, they are expressed in tensorial form and hence can be easily implemented into computer programmes. As regards eqn (18), in particular, since the material constants involved can be determined from the usual creep tests under constant uniaxial tension, it may be a promising constitutive equation for practical analyses of engineering problems of creep.

Acknowledgement—The authors wish to express their gratitude to Prof. Y. Ohashi of Nagoya University for his valuable advice and encouragement.

REFERENCES

1. F. K. G. Odqvist and J. Hult, *Kriechfestigkeit metallischer Werkstoffe*. Springer, Berlin (1962).
2. Yu. N. Rabotnov, *Creep Problems of Structural Members*. North-Holland, Amsterdam (1969).
3. H. Kraus, *Creep Analysis*. Wiley, New York (1980).
4. J. Gittus, *Creep, Viscoelasticity and Creep Fracture in Solids*. Applied Science, London (1975).
5. J. M. Corum, W. L. Greenstreet, K. C. Liu, C. E. Pugh and R. W. Swindeman, Interim guidelines for detailed inelastic analysis of high-temperature reactor system components. ORNL-5014, Oak Ridge National Laboratory, Tennessee (1974).
6. S. Murakami, H. Kumazaki and K. Tamaki, Experimental study on creep of type 304 stainless steel under variable stress. Preprint of JSME, No. 813-1, 24 (1981).
7. Y. Ohashi, N. Ohno and M. Kawai, Evaluation of creep constitutive equations for type 304 stainless steel under repeated multiaxial loading. *ASME J. Engng Mat. Tech.*, to be published.
8. M. Ohnami, K. Motoie and N. Yoshida, Study on the influence of strain history on creep of polycrystalline metallic materials at elevated temperature. *Zairyo* **18**, 226 (1969).

9. J. J. Blass and W. N. Findley, Short-time, biaxial creep of an aluminum alloy with abrupt change of temperature and state of stress. *ASME J. Appl. Mech.* **38**, 489 (1971).
10. Z. Mróz, An attempt to describe the behaviour of metals under cyclic loads using a more general workhardening model. *Acta Mech.* **7**, 199 (1969).
11. M. A. Eisenberg and A. Phillips, A theory of plasticity with non-coincident yield and loading surfaces. *Acta Mech.* **11**, 247 (1971).
12. Y. F. Dafalias and E. P. Popov, Plastic internal variables formalism of cyclic plasticity. *ASME J. Appl. Mech.* **43**, 645 (1976).
13. R. D. Krieg, A practical two surface plasticity theory. *ASME J. Appl. Mech.* **42**, 641 (1975).
14. R. Lagneborg, A theoretical approach to creep deformation during intermittent load. *ASME J. Basic Engng* **93**, 205 (1971).
15. R. D. Krieg, J. C. Swearengen and R. W. Rohde, A physically-based internal variable model for rate-dependent plasticity. *Inelastic Behavior of Pressure Vessel and Piping Components* (Edited by T. Y. Chang and E. Krempl), p. 15. ASME, New York (1978).
16. N. N. Malinin and G. M. Khadjinsky, Theory of creep with anisotropic hardening. *Int. J. Mech. Sci.* **14**, 235 (1972).
17. J. L. Chaboche, Viscoelastic constitutive equations for the description of cyclic and anisotropic behaviour of metals. *Bull. Acad. Polon. Sci., Ser. Sci. Tech.* **25**, 33 (1977).
18. A. Miller, An inelastic constitutive model for monotonic, cyclic and creep deformation. *ASME J. Engng Mat. Tech.* **98**, 97 (1976).
19. J. L. Chaboche, K. Dang Van and G. Cordier, Modelization of the strain memory effect on the cyclic hardening of 316 stainless steel. *Trans. 5th Int. Conf. Struc. Mech. Reactor Tech.* (Edited by T. A. Jaeger and B. A. Boley), North-Holland, Amsterdam (1979).